Probing the Dark State Tertiary Structure in the Cytoplasmic Domain of Rhodopsin: Proximities between Amino Acids Deduced from Spontaneous Disulfide Bond Formation between Cysteine Pairs Engineered in Cytoplasmic Loops 1, 3, and 4

Kewen Cai,[§,||] Judith Klein-Seetharaman,[§,⊥] Christian Altenbach,[#] Wayne L. Hubbell,[#] and H. Gobind Khorana*[,§]

Departments of Biology and Chemistry, Massachusetts Institute of Technology, 77 Massachusetts Avenue, Room 68-680, Cambridge, Massachusetts 02139, and Jules Stein Eye Institute and Department of Chemistry and Biochemistry, University of California, Los Angeles, California 90095

Received April 12, 2001; Revised Manuscript Received July 30, 2001

ABSTRACT: To probe proximities between amino acids in the cytoplasmic domain by using mutants containing engineered cysteine pairs, three sets of rhodopsin mutants have been prepared. In the first two sets, a cysteine was placed, one at a time, at positions 311−314 in helix VIII, while the second cysteine was fixed at position 246 (set I) and at position 250 (set II) at the cytoplasmic end of helix VI. In the third set, one cysteine was fixed at position 65 while the second cysteine was varied between amino acid positions 306 and 321 located at the cytoplasmic end of helix VII and throughout in helix VIII. Rapid disulfide bond formation in the dark was found between the cysteine pairs in mutants A246C/Q312C,-A246C/K311C and in mutants H65C/C316, H65C/315C and H65C/312C. Disulfide bond formation at much lower rates was found in mutants A246C/F313C, V250C/Q312C, H65C/N310C, H65C/K311C, H65C/F313C, and H65C/R314C; the remaining mutants showed no significant disulfide bond formation. Comparisons of the results from disulfide bond formation in solution with the distances observed in the rhodopsin crystal structure showed that the rates of disulfide bond formation in most cases were consistent with the amino acid proximities as revealed in crystal structure. However, deviations were also found, in particular, in the set containing fixed cysteine at position Cys246 and cysteines at positions 311−314. The results implicate significant effects of structural dynamics on disulfide bond formation in solution.

Recent work on rhodopsin, the vertebrate rod cell photoreceptor, has shown that there is coupling in in vivo folding between packing of the seven helices to form the transmembrane (TM)[1] domain and folding of the intradiscal domain (ID) to a unique tertiary structure. The two important consequences of this process are the formation of a precise pocket where 11-*cis*-retinal binds and the folding of the cytoplasmic domain (CP) to the dark state tertiary structure. Subsequent light-catalyzed isomerization of the retinal results in a conformational change that initiates visual transduction (*2*−*5*). Molecular description of the dark and the light-activated structures are the long-range goals of structural work on rhodopsin. To probe the dark state tertiary structure, we have taken an approach that aims at determining proximities between amino acids in different regions of the CP domain by introducing pairs of cysteines at the sites of the original amino acids and measuring spontaneous disulfide bond formation between the cysteine pairs. The total sets of rhodopsin double cysteine mutants that have been studied are listed in Table 1. Here we explore the spatial relationships between the cytoplasmic ends of TM helices I, VI, and VII. Earlier work has suggested the involvement of the cytoplasmic ends of helices VI and VII in a tertiary structure which is recognized by G_T after light-activation (*6*−*8*). Further, a structural change in these two helices upon illumination of rhodopsin has been shown previously (*4*, *5*, *9*). However, the relative topology of the cytoplasmic ends of helix VII with respect to CL1 and CL3 in the dark and its change after light-activation remain unclear. We now have studied three sets of rhodopsin mutants (Figure 1, Table 1). In the first two sets, a cysteine was placed, one at a time, at positions 311−314 at the end of helix VII, while the second cysteine

[†] This work was supported by NIH Grants GM28289 and EY 11716 (H.G.K.) and EY05216 (W.L.H.), the Jules Stein Professorship endowment (W.L.H.), and a grant from the Ford Bundy and Anne Smith Bundy Foundation. K.C. was supported by the MIT Department of Chemistry Cancer Training Grant CA 09112. J.K-S. was the recipient of a Howard Hughes Predoctoral Fellowship.

[‡] This is paper 47 in the series "Structure and Function in Rhodopsin". Preceding paper in this series is ref *1*.

* To whom correspondence should be addressed. Phone: (617) 253-1871. Fax: (617) 253-0533. E-mail: khorana@mit.edu.

[§] Departments of Biology and Chemistry, Massachusetts Institute of Technology, 77 Massachusetts Avenue, Cambridge, MA 02139.

[||] Present address: Biogen, Inc. 14 Cambridge Center, Cambridge, MA 02l42.

[⊥] Present address: Institute for Software Research International, Department of Computer Science, Carnegie Mellon University, Wean Hall 4604, Pittsburgh, PA 15213.

[#] Jules Stein Eye Institute and Department of Chemistry and Biochemistry, University of California, Los Angeles, CA 90095.

[1] Abbreviations: DM, dodecylmaltoside; CP, cytoplasmic domain; TM, transmembrane; ID, intradiscal; 4-PDS, 4,4′-dithiodipyridine; Meta II, metarhodopsin II; WT, wild-type; CL1, CL2, CL3, CL4, cytoplasmic sequences connecting TM helices I and II, III and IV, V and VI, VII and the palmitoylation sites, respectively; H8, helix in CL4.

10.1021/bi010747h CCC: $20.00
Published on Web 09/27/2001

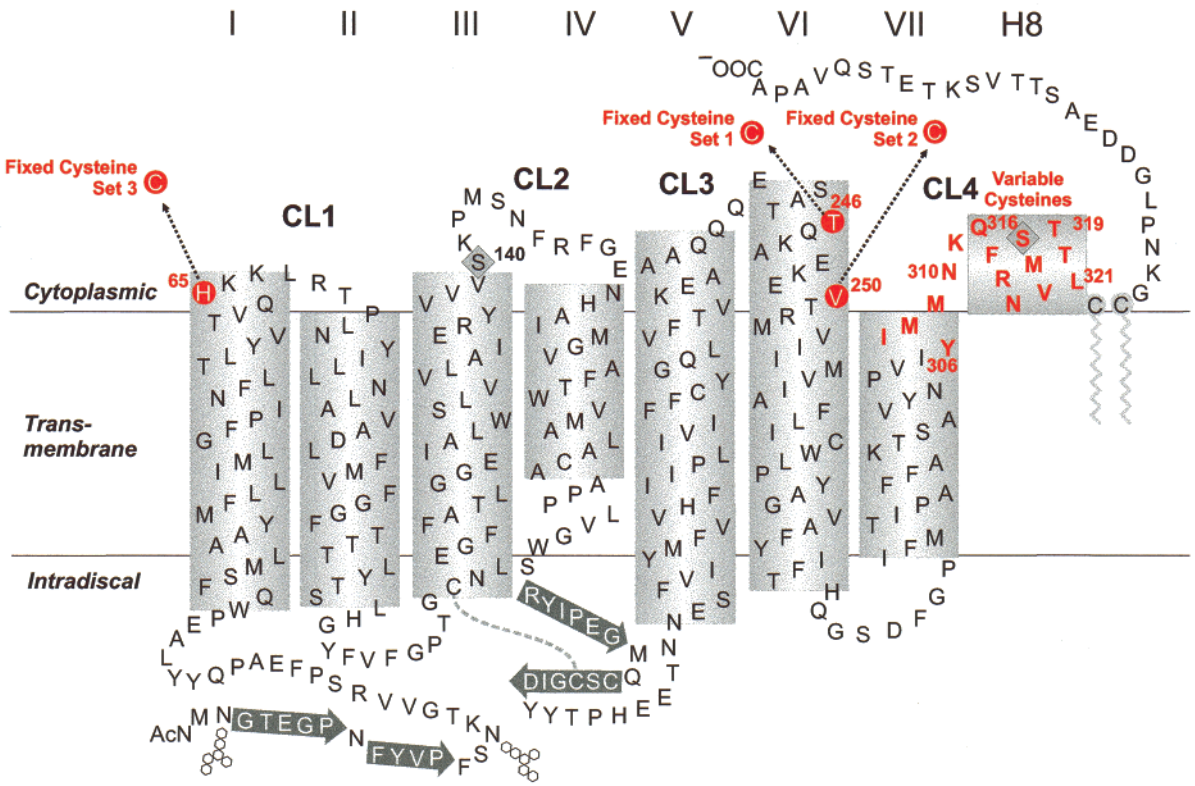

FIGURE 1: Secondary structure model of bovine rhodopsin shows the double cysteine replacements in the cytoplasmic domain made in this work. Transmembrane helices are designated I to VII. CP loops are designated CL1−CL4. The helix in CL4, which was observed in the crystal structure (*10*), is designated H8. The gray arrows indicate the amino acid sequences containing the β-sheet structure. Three sets of double mutants are shown in red with the constant cysteine at position 246 (set I), 250 (set II), and 65 (set III), respectively.

Table 1: Sets of Cysteine Pairs Studied for Proximity Relationships in the Tertiary Structure of the Cytoplasmic Face of Rhodopsin

cysteine pairs		disulfide bond formed most rapidly	ref
cysteine I (fixed)	cysteine II (varied)		
Cys65	Cys306 to Cys321	Cys65−Cys316	this work
Cys246	Cys311to Cys314	Cys246−Cys312	this work
Cys250	Cys311 to Cys314	Cys250−Cys312	this work
Cys316	Cys60 to Cys74	Cys65−Cys316	*1*, *6*
Cys139	Cys247 to Cys252	Cys139−Cys250; Cys139−Cys248[a]	*5*
Cys338	Cys240 to Cys250; Cys65; Cys140	Cys245−Cys338	*11*

[a] On the basis of EPR studies, these two cysteine pairs exhibited the strongest spin−spin interactions.

was fixed at position 246 in one set and at position 250 in the second set, CP end of TM VI. In the third set, one cysteine was fixed at position 65 while the second cysteine was varied between amino acids 306 and 321 at CP end of TM VII and helix VIII. Spontaneous disulfide bond formation was studied in all the mutants under identical conditions. Rapid disulfide bond formation in the dark was found between the cysteine pairs in mutants A246C/Q312C and A246C/K311C and in the pairs H65C/C316, H65C/315C, and H65C/312C. Disulfide bond formation at much slower rates was found in mutants A246C/F313C, V250C/Q312C, H65C/N310C, H65C/K311C, H65C/F313C, and H65C/R314C while the remaining mutants showed no significant disulfide bond formation. Comparison of the above proximity results obtained in solution with the distances observed in the rhodopsin crystal structure shows that the rates of disulfide bond formation in most cases are as expected. However, deviations are also observed, in particular, in the set containing Cys246 and cysteines at positions 311−314. The results implicate significant effects of structural dynamics on disulfide bond formation.

MATERIALS AND METHODS

All materials used were as described in the previous paper in this issue (*1*). Buffers used were buffer A, 137 mM NaCl, 2.7 mM KCl, 1.8 mM KH_2PO_4, 10 mM $NaHPO_4$ (pH 7.2); buffer B, buffer A plus 1% (wt/vol) DM, 2 mM ATP and 2 mM $MgCl_2$, 0.1 mM phenylmethanesulfonyl fluoride (PMSF); buffer C, buffer A plus 0.05% DM (wt/vol); buffer D, 5 mM 2-(*N*-morphholino)ethanesulfonic acid (MES), pH 6.0, 0.05% DM (wt/vol); buffer E, 2 mM NaPi, pH 7.5, 0.05% DM (wt/vol); buffer F, buffer E plus 1 mM DTT; buffer G, 50 mM NaPi (pH 7.6), 0.05% DM.

Construction of Double Cysteine Rhodopsin Mutants. The two sets of mutants, A246C/K311C to A246C/R314C and V250C/K311C to V250C/R314C, were prepared from the corresponding single cysteine mutants K311C to R314C (*7*) by using fragment replacement mutagenesis. The mutants A246C/K311C to A246C/R314C were constructed from the previously constructed mutant A246C/S338C (*9*) by replacing the restriction fragment *Mlu*I/*Nhe*I (1876 bp) in plasmid A246C/S338C with the fragment *Mlu*I/*Nhe*I (1876 bp) from the corresponding single cysteine mutants (K311C−R314C). Similarly, mutants V250C/K311C to V250C/R314C were produced by replacing the *Mlu*I/*Nhe*I fragment (1876 bp) of plasmid V250C/S338C (*9*) with fragment *Mlu*I/*Nhe*I (1876 bp) from the single cysteine plasmids, K311C to R314C.

Table 2: Characterization of Double Cysteine Substitution Mutants

mutant	chromophore λ_{max} (nm)	A_{280}/A_{500}[a]	Meta II decay[b] ($T_{1/2}$, min)	no. of free sulfhydryl groups
WT	500	1.6	11.2 (11.5)[c]	2
set I				
A246C/K311C	500	1.7	11.4 (11.4)	2
A246C/Q312C	500	1.7	7.1 (11.4)	2
A246C/F313C	498	1.8	14.1 (13.1)	2
A246C/R314C	500	1.7	15.1	2
set II				
V250C/K311C	501	1.7	12.6	2
V250C/Q312C	500	1.7	13.6 (11.4)	2
V250C/F313C	500	1.7	13.9	2
V250C/R314C	500	1.7	14.7	2
set III				
H65C/Y306C	500	1.6	17.8	2
H65C/I307C	500	1.7	9.2	2
H65C/M308C	499	1.6	8.7	2
H65C/M309C	498	1.6	8.5	2
H65C/N310C	500	1.7	14.1	2
H65C/K311C	499	1.6	8.7	2
H65C/Q312C	499	1.6	12.2	2
H65C/F313C	497	1.8	12.6	2
H65C/R314C	497	1.7	13.1	2
H65C/N315C	499	1.6	10.5	2
H65C/316C	499	1.6	11.4	2
H65C/M317C	500	1.9	11.4	2
H65C/V318C	500	1.9	10.2	2
H65C/T320C	500	2.0	9.6	2
H65C/L321C	500	2.1	9.5	2

[a] Ratios determined at pH 6. [b] The values in brackets are after DTT treatment.

The double cysteine mutants, H65C/Y306C to H65C/L321C, were derived from the previously described (*7*) corresponding single cysteine mutants Y306C to L321C.

These single cysteine mutants contain replacements in the sequence 306−321 one at a time. The double cysteine mutants were prepared from the single cysteine mutant H65C (*12*). The restriction fragment *Pst*I/*Sal*I (304 bp) of this plasmid was replaced by *Pst*I/*Sal*I fragment (304 bp) from the single cysteine mutants Y306C to L321C.

In all double cysteine mutants, Cys140 and Cys316 were replaced by serines unless indicated otherwise. The sequences of the mutants following mutations were confirmed by the dideoxynucleotide sequencing method (*13*).

Determination of the Rates of Disulfide Bond Formation. Rhodopsin mutants were all eluted from 1D4-Sepharose with buffer D and the concentration of each mutant was adjusted to 2.5 μM with the same buffer. The pH of the samples was then raised to 7.7 by adding 0.5 M Na_2HPO_4 buffer (pH 9.2). The time courses of disulfide bond formation were monitored by taking aliquots (36 μL) at different time intervals for titration with 4-PDS as described previously (*11*). The decrease in the amount of the free −SH groups in the double cysteine mutants indicated the extent of disulfide bond formation at that time point (*9*). All buffers used for determination of disulfide bond formation rates were purged with Argon.

UV−Vis Absorption Spectroscopy and Measurements of Meta II Decay Rates. UV−Vis absorption spectra were recorded using a Perkin-Elmer λ-7 spectrophotometer. Meta II decay rates of the rhodopsin mutants were measured in buffer E by the fluorescence increase assay (*14*). To measure the decay rates of Meta II in sulfhydryl forms of the mutants, the samples were preincubated with 1 mM DTT for 1 h at room temperature. Rates were then measured in buffer F.

RESULTS

Characterization of the Double Cysteine Mutants of Rhodopsin. (a) Expression and Spectral Properties. All the three sets of mutants, A246C/K311C to A246C/R314C, V250C/K311C to V250C/R314C, and H65C/Y306C to H65C/L321C, were expressed in COS 1 cells, immunopurified and isolated at pH 6 as described (*11*). The yields of the purified expressed mutants were comparable to that of expressed WT rhodopsin. All of the expressed opsins formed typically rhodopsin chromophore, with λmax 498 nm to 500 nm after reconstitution with 11-*cis*-retinal. The UV−vis absorbance rations, A_{280}/A_{500}, in all cases were in the range 1.6 and 2.1 (Table 2). Thus, as found earlier for the corresponding single cysteine mutants (*6*, *7*), introduction of second cysteine residues in the cytoplasmic region of rhodopsin did not affect the correct folding and spectral properties of the expressed proteins.

(b) Characterization of Metarhodopsin II formation: Upon illumination, all mutants formed a Meta II intermediate as seen by the spectral shift from λ_{max}, ~500 nm to λ_{max}, 380 nm after bleaching. The decay rates of Meta II, as measured by the fluorescence increase method, showed that $T_{1/2}$ ranged from 8.4 to 17.8 min, compared to 10.5 min for WT rhodopsin under the conditions used (Table 2). Thus, majority of the mutants showed normal decay rates, while significant increase in $T_{1/2}$ was observed for the mutant H65C/Y306C, and a significant decrease for the mutant A246C/Q312C. For the four mutants that showed disulfide bond formation, Meta II decay rates were also measured under reducing conditions by addition of DTT. WT rhodopsin and the mutants A246C/K311C, A246C/F313C, and V250C/Q312C showed no significant change in Meta II decay rate on DTT treatment. However, mutant A246C/Q312C showed considerable de-

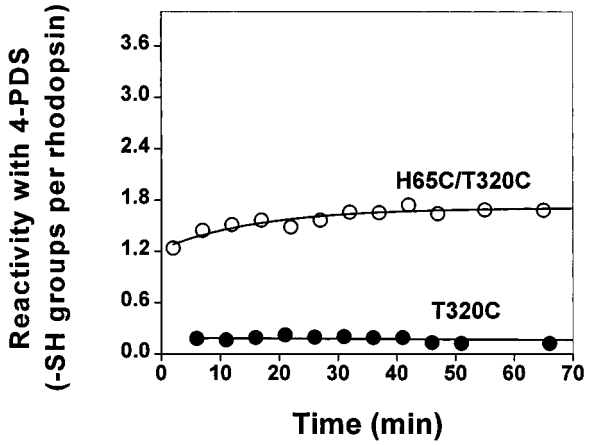

FIGURE 2: Reaction time courses of mutants T320C (solid circle) and H65C/T320C (open circle) with 4-PDS. The reactions were recorded by monitoring the development of absorbance of thiopyridone at 323 nm as described in the Materials and Methods. The number of reacted cysteines (mole of −SH per mole of rhodopsin), and thus the reaction extent, is plotted as a function of time.

crease in Meta II half-life in the disulfide-bonded form (7.1 min). On reduction, the value increased to 11.4 min, similar to that of WT rhodopsin.

(c) Quantitation of Sulfhydryl Groups in Cysteine Mutants. Titrations with 4-PDS showed that all the double cysteine mutants, when freshly purified and kept at pH 6, contained nearly two reactive sulfhydryl groups in the dark (Table 2). In every case, derivatizations with 4-PDS went to completion in under 15 min. In particular, it is of interest to note that while both cysteines in the mutants H65C/M317C, H65C/V318C, H65C/T320C, and H65C/L321C, invariably reacted rapidly with PDS, the corresponding single cysteine mutants at the positions 317, 318, 320, and 321, were found previously to show almost no reactivity with PDS (*7*). Comparison of reaction kinetics with PDS is shown in Figure 2 for the single cysteine mutant T320C and the corresponding double cysteine mutant, T320C/H65C.

Disulfide Bond Formation in Double Cysteine Mutants. The pH of the solutions of the double cysteine mutants was raised from 6 to 7.7 and the spontaneous disulfide bond formation was followed, on storage at room temperature, by the decrease in free sulfhydryl groups by titration with 4-PDS.

Figure 3A shows the extent of disulfide bond formation as a function of time for three mutants selected from the first two sets of mutants. As seen, the rates of disulfide bond formation varied. Thus, disulfide bond formation was influenced by both the position of cysteine in CL3 as well as the cysteine position in helix VIII. The rates of disulfide bond formation for all the eight mutants in the two sets are compared in Figure 3B. Rapid disulfide bond formation was observed only with mutants A246C/K311C and A246C/Q312C, with $T_{1/2}$ of 4.2 and 3.8 h, respectively. Mutants A246C/F313C and V250C/Q312C showed much slower rates of disulfide bond formation with $T_{1/2}$ of 19 and 42 h, respectively. No disulfide bond was detected in mutants A246C/R314C, C250C/K311C, V250C/F313C, and V250C/R314C.

In the third set of double cysteine mutants involving H65C and cysteines at positions 306−321, disulfide bond formation

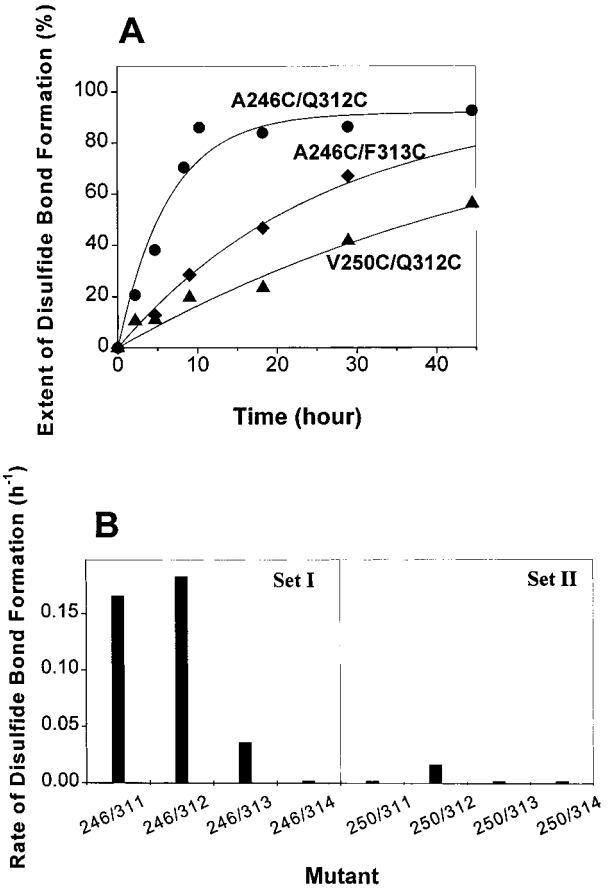

FIGURE 3: Disulfide bond formation in double cysteine mutants A246C/K311C−A246C/R314C (set I) and V250C/K311C−V250C/R314C (set II). All the mutants were eluted from the immunoaffinity column at pH 6.0, and then shifted to pH 7.7 as described in the Materials and Methods. The extent of disulfide bond formation was monitored by the decrease in sulfhydryl groups over the time by reaction with 4-PDS (Materials and Methods). Time-courses of disulfide bond formation in mutants A246C/Q312C (circle), A246C/F313C (diamond) and V250C/Q312C (triangle). Comparison of the rates of disulfide bond formation in mutants set I and set II. The rate constant of each mutant ($hour^{-1}$) was obtained by single-exponential curve fitting of the time course of disulfide bond formation as shown in panel A.

was complete in H65C/C316 within 4.5 h and the mutant H65C/N315C also showed relatively rapid disulfide formation (Figure 4A). However, the rates of disulfide bond formation for H65C/Q312C and H65C/K314C were much slower. Figure 4B compares disulfide bond formation rates for all of the double cysteine mutants in this set. Thus, the mutant H65C/316C showed the most rapid disulfide formation, while no disulfide bond formation was detected for mutants H65C/Y306C to H65C/M309C nor for mutants H65C/M317C to H65C/L321C.

DISCUSSION

Qualitative evidence for the presence of a dark state tertiary structure in the CP domain of rhodopsin has been forthcoming from a number of previous studies. In the present series of papers (Table 1), we have sought more definitive information on the structure by probing proximity relationships between amino acids in different regions of the CP domain. The approach uses rhodopsin in which pairs of amino acids in the native structure are replaced by cysteines.

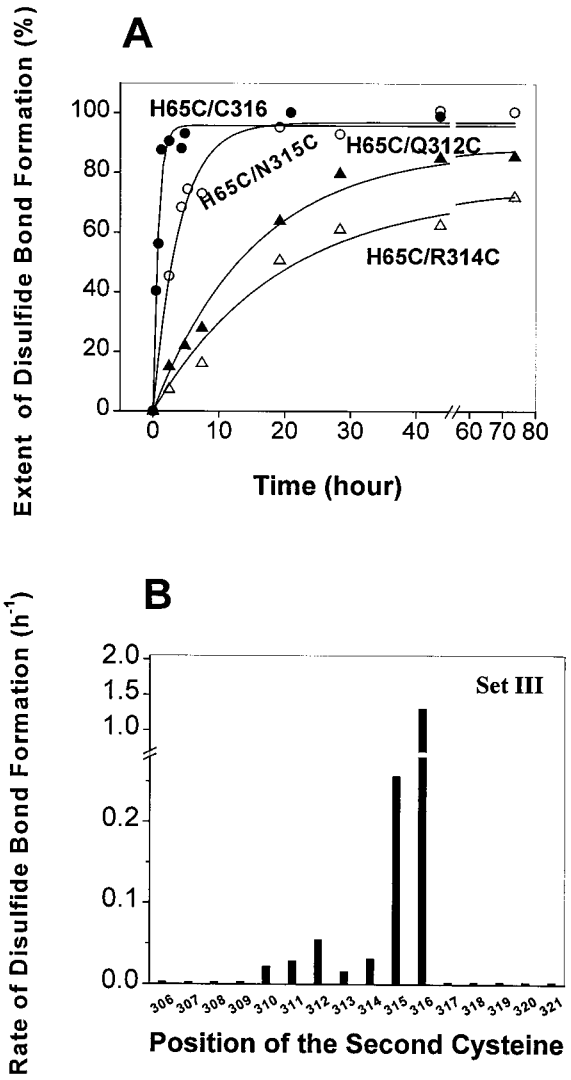

FIGURE 4: Disulfide bond formation in double cysteine mutants H65C/Y306C−H65C/L321C (set III). Kinetics was determined as described in the Materials and Methods. Time courses of disulfide bond formation between Cys65 and select cysteines (316, solid circle; 315, open circle; 312, solid triangle; 314, open triangle). (B) Comparison of the rates obtained by single-exponential curve fitting of the time course of disulfide bond formation as shown in panel A.

Spontaneous disulfide bond formation between the cysteines reflects proximity between the original amino acids. Complementary to the work described earlier (Table 1) and in the previous paper in this issue (*1*), the present work focuses on the topology of CL4 in relation to CL1 and CL3, using the three sets of di-cysteine mutants described above. The recent availability of a three-dimensional model of rhodopsin based on X-ray crystallographic analysis (*10*) allows a comparison of proximities between amino acids deduced in solution with the crystal structure (Figure 5). The double cysteine replacements were introduced into the crystal structure model using the InsightII program as described in the previous paper in this issue and the distances between the sulfurs in the two cysteines were measured. The reciprocal of these distances was plotted together with the rates of disulfide bond formation (Figure 6).

The topology of CL4 in the crystal and the positions of the cysteines fixed at positions 246, 250, and 65 in the three di-cysteine sets is shown in Figure 5A. The presence of an

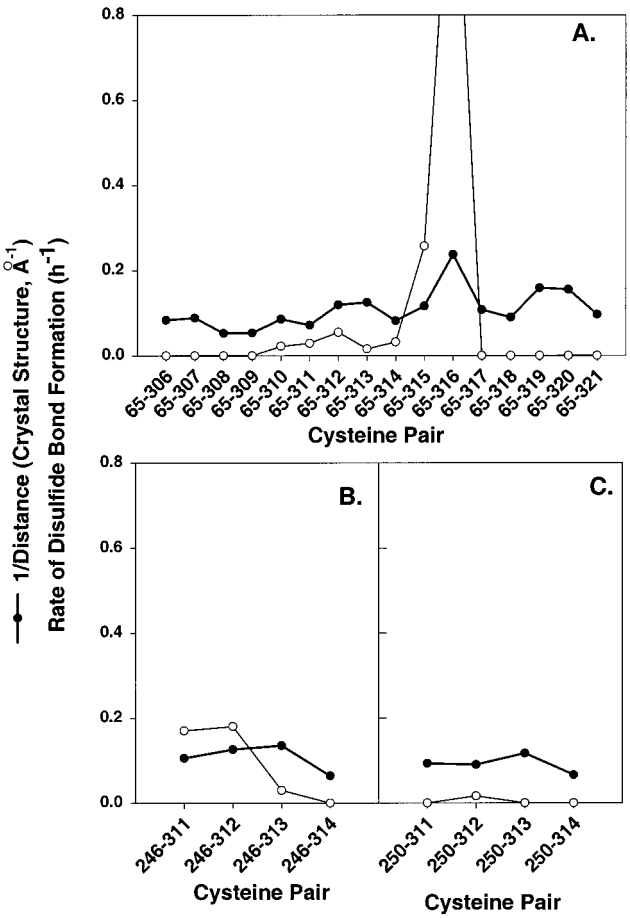

FIGURE 5: Proximity between His65, Phe313, Lys311, V250, and A246. Positions of the residues in the crystal structure. Distance between cysteine pairs in double cysteine mutants. (I) Cys65/Cys313. (II) Cys246/Cys313. (III) Cys246/Cys311.

α-helix, the eighth helix, H8, in CL4 has been a striking finding from the crystal structure. H8, being perpendicular to the TM helical bundle, is oriented toward the outside of the bundle and continues until the palmitoylation anchoring sites. Thus, although TM helix VII is neighbor to TM helices I, II, and VI, CL4 itself turns away from TM helix VI along with TM helices I and II to the outside of the helical bundle (Figure 5A). The transition between TM helix VII and H8 in CL4 is provided by a turn composed of residues 311 and 312, while all the C-terminal residues after Gln312 are located on a stable secondary structure element facing away from TM helix VI.

We first discuss disulfide cross-links observed in the double cysteine sets in which one cysteine varied between positions 311 and 314 and the second cysteine was fixed at position 246 (set I, Table 2) or at position 250 (set II, Table 2).

The topology of cysteines at positions 246 and 250 is well-defined. Both previous EPR data and the crystal structure are in close agreement regarding these residues and place 250 in the central cavity of the TM helix bundle facing TM helices II and III, where it is immobilized. Residue 246 faces TM helix VII, but lies above the transition between TM helix VII and H8. Thus, cysteine at position 246 has high solvent accessibility and mobility (*4*). Of the two cysteines at positions 246 and 250, only the cysteine at position 246 can form disulfide bonds with cysteines at positions 311−314.

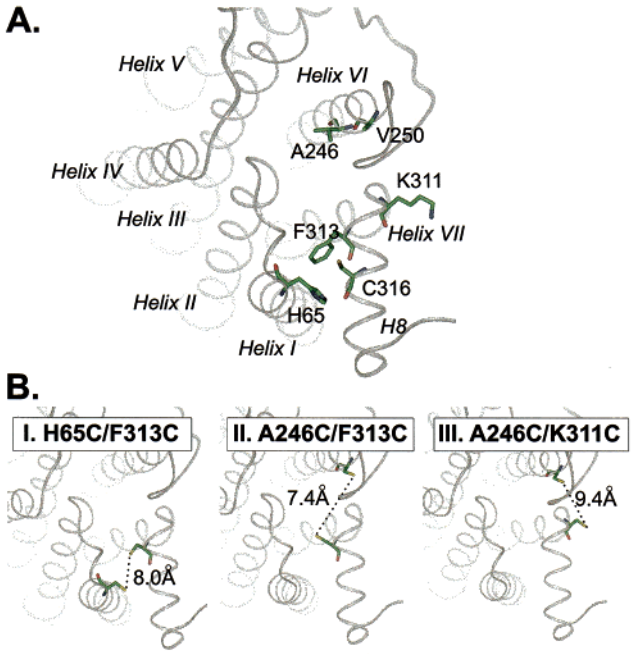

FIGURE 6: Comparison of disulfide bond formation rates in the three sets of double cysteine mutants with inverse distances obtained from the crystal structure of rhodopsin (*10*). Open circles: disulfide bond formation rates. Closed circles: Reciprocal of distances from Sγ to Sγ of the two cysteines.

Thus, although the distances between the di-cysteine pairs in both sets I and II are very similar, very little or no disulfide bonds are formed with Cys250 (Figure 6C). Proximity alone is insufficient to explain the disulfide bonding data in this region. Rather, the lack of disulfide bond formation with Cys250 reflects its immobilization and rigidity in the cavity of the TM helical bundle. While, as mentioned above, Cys246 can form disulfide bonds, based on proximity alone sites 311−313 would be expected to form disulfide bonds equally well (Figure 6B). However, there is a sharp decrease in disulfide bonding rate from 312 to 313, and no disulfide bond formed with 314. This result agrees well with the topology of CL4 in the crystal, namely that 313 is part of a stable secondary structure element in H8, while 311 and 312 are loop residues that connect TM helix VII with CL4. Consistent with the immobilization of 313 in H8 are the previous EPR mapping data where it was concluded that 313 is buried and rigid. Formation of a disulfide bond between 246 and 313 thus requires significant distortion, and disulfide bonds form very slowly (Figure 6B). Further distortion of H8 in CL4 seems impossible, as shown by the lack of disulfide bond formation with residue 314. The result indicates that H8 in CL4 is very stable and does not melt to allow disulfide bonds to form.

The stability of H8 in CL4 described above is further supported by the results with the di-cysteine mutants with one cysteine fixed at position 65 and the second cysteine varied from 306 to 321. Clearly, there is a periodicity in distances between residues 311 and 321 with respect to Cys65, with minimal distances for 312/313, 315−317, and 319/320 (Figure 6A). However, only very few disulfide bonds formed. Rapid disulfide bond formation was observed between Cys65 with Cys315 and Cys316 while slow disulfide bond formation occurred also with Cys312 (Figure 6A). Other disulfide bonds, expected on the basis of proximity alone, did not form. These results contrast with those from the set of di-cysteine mutants described in the previsou paper in this issue (ref *1*, Figure 5), in which periodicity in proximity was well matched by periodicity in disulfide bond formation.

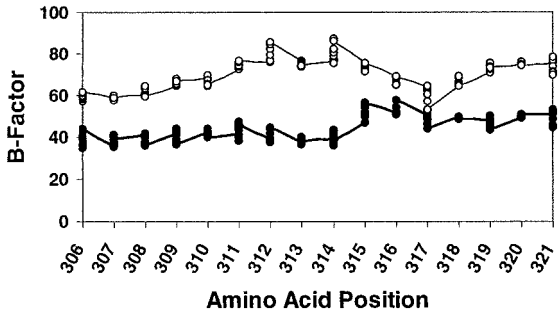

FIGURE 7: Temperature factors as a function of amino acid position in the region 306−321. The temperature factors were obtained from the rhodopsin crystal structure coordinate file 1F88 (*10*). Since rhodopsin was modeled as a dimer, two sets of temperature factors were reported and are plotted here.

Thus, comparison of the rates of disulfide bond formation in the present set, Cys65 and Cys306−321, with that in the set Cys316 and Cys61−74 demonstrates the balance between proximity and steric immobilization in disulfide bond formation. The lack of correlation observed between proximity and disulfide bond formation in the present set is further supported by the EPR data (C.A., K.C., J.K.-S., H.G.K., and W.L.H., unpublished work). Strongest spin−spin interaction was observed between residues 65 and 319, but no disulfide bonds form between them. Further emphasis for this notion comes from an analysis of the temperature factors reported in the recent rhodopsin crystal structure (*10*). These are shown in Figure 7 as a function of amino acid position in the region 306−321. While the temperature-factor values are overall similar, local maxima at 312 and 314, and a local minimum at 317 were observed (Figure 7). These differences in mobility appearing in the crystal structure may be part of the reason the periodicity in proximity observed in the crystal is not represented by a similar periodicity in the disulfide bond formation rates. However, the refinement of the crystal structure is low (2.8 Å) and limits the reliability of the temperature factors.

The impact of structure in CL4 on the reactivity of cysteines in the single cysteine mutants, Cys306 to Cys321 (*4*), and in corresponding to the double cysteine mutants (set 3, Table 2) proved to be striking. Previously, the single cysteine mutants, M317C, C318C, T320C, and L321C, were inert both to 4-PDS and to the nitroxide spin labeling reagent. However, in the present double cysteine set of mutants, both cysteines were reactive to 4-PDS throughout.

The position of residues 316−321 with respect to 65 is shown in Figure 8. Cys316 and Cys319 are highly reactive, both, in the presence or absence of cysteine at position 65. These two residues face toward TM helices I and II, but lie above CL1, being very solvent exposed. In contrast, all other residues in the sequence 316−321 in H8 of CL4 face the lipid phase. Their reactivity is low, presumably due to the suppression of ionization of the sulfhydryl group and the low solubility of 4-PDS in the lipid phase (*15*). Why do these cysteines react when a cysteine is also present at position 65? One possibility is that Cys65 perturbs the structure in a

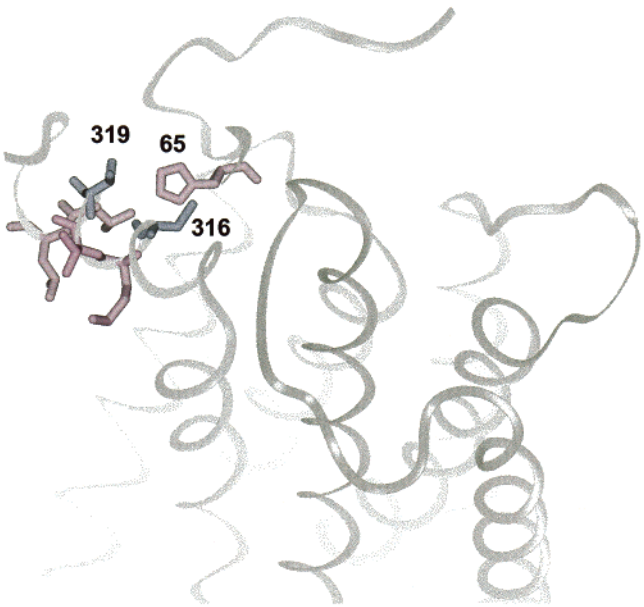

FIGURE 8: Positions of residue 316−321 (CL4) and 65 (CL1) in the crystal structure model (*10*). The reactivity of cysteine at position 316 and 319 (shown in blue) is independent of the replacement of His65 (shown in red) by cysteine. However, cysteines at all other positions in this region (317, 318, 320, 321), which are shown in red, showed reactivity only if His65 is replaced with cysteine.

way that allows the reaction of the cysteines in H8. This is consistent with the apparent tight packing in this region (*4*, *8*) and the low reactivity to form disulfide bonds discussed above. Thus, the interaction of His65 with Cys316 is visible in the crystal, in which these two residues are in H-bonding distance, and is supported by the ability to form a disulfide bond the fastest in all sets studied to date (Table 1). Removal of such interaction by cysteine substitution would significantly loosen the position of H8 in CL4, as to allow reaction with 4-PDS. However, a second possibility is as follows. Cys65 is a very reactive cysteine. It is possible that Cys65 reacts fast in the di-cysteine set studied here, increasing the effective concentration of thiopyridinyl disulfide. Thus, after the reaction of 4-PDS with Cys65, the reaction of the mixed disulfide with the second cysteine will be much faster due to local concentration effects.

In summary, disulfide bond formation has been studied comprehensively as an indicator of proximity between amino acids in rhodopsin CP domain tertiary structure. The results obtained in solution have been compared with the static crystal structure. These highlight the fine balance between proximity and structural factors, e.g., steric immobilization in determining the rates of disulfide bond formation. Modeling of the engineered cysteines in the crystal structure indicates that small but significant motions are required for productive disulfide bond formation. During these motions, secondary structure elements are retained as demonstrated by the lack of disulfide bond formation in cysteines that do not face toward each other in the crystal structure model. Such motions may be important in allowing light-induced motions to occur.

ACKNOWLEDGMENT

We thank Professor U. L. RajBhandary of the Biology Department of the Massachusetts Institute of Technology and members of this laboratory for helpful discussions. Ms. Judy Carlin's assistance during the preparation of the manuscript is gratefully acknowledged.

REFERENCES

1. Seetharaman, J. K., Hwa, J., Cai, K., Altenbach, C., Hubbell, W. L., and Khorana, H. G. *(2001) Biochemistry*, 12472-12478.
2. Khorana, H. G. (1992) *J. Biol. Chem. 267*, 1−4.
3. Farahbakhsh, Z. T., Ridge, K. D., Khorana, H. G., and Hubbell, W. L. (1995) *Biochemistry 34*, 8812−8819.
4. Altenbach, C. A., Yang, K., Farrens, D. F., Khorana, H. G., and Hubbell, W. L. (1996) *Biochemistry 35*, 12470−12478.
5. Farrens, D. L., Altenbach, C., Yang, K., Hubbell, W. L., and Khorana, H. G. (1996) *Science 274*, 768−770.
6. Yang, K., Farrens, D. L., Hubbell, W. L., and Khorana, H. G. (1996) *Biochemistry 35*, 12464−12469.
7. Cai, K., Seetharaman, J. K., Farrens, D., Cheng, Z., Altenbach, C. A., Hubbell, W. L. and Khorana, H. G. (1999), *Biochemistry 38*, 7925−7930.
8. Cai, K., Seetharaman, J. K. Hwa, J., Hubbell, W. L., and Khorana, H. G. (1999) *Biochemistry 38*, 12893−12898.
9. Altenbach, C., Cai, K., Khorana, H. G., and Hubbell, W. L. (1999) *Biochemistry 38*, 7931−7937.
10. Palczewski, K., Kumasaka, T., Hori, T., Behnke, C. A., Motoshima, H., Fox, B. A., LeTrong, I., Teller, D. C., Okada, T., Stenkamp, R. E., Yamamoto, M., and Miyano, M. (2000) *Science 289*, 739−745.
11. Cai, K., Langen, R., Hubbell, W. L., and Khorana, H. G. (1997) *Proc. Natl. Acad. Sci. U.S.A. 94*, 14267−14272.
12. Yang, K., Farrens, D. L., Altenbach, C., Farahbakhsh, Z. T., Hubbell, W. L., and Khorana, H. G. (1996) *Biochemistry 35*, 14040−14046.
13. Sanger, F., Nicklen, S., and Coulson, A. R. (1977) *Proc. Natl. Acad. Sci. U.S.A.* 74, 5463−5467.
14. Farrens, D. L., and Khorana, H. G. (1995) *J. Biol. Chem. 270*, 5073−5076.
15. Chen, Y. S., and Hubbell, W. L. (1978) *Membr. Biochem. 1*, 107−129.

BI010747H